Materials Chemistry and Physics 259 (2021) 124101

Contents lists available at ScienceDirect

Materials Chemistry and Physics

journal homepage: www.elsevier.com/locate/matchemphys

Preparation of a novel lignin-based flame retardant for epoxy resin

Dingxiang Liang [a], Xiaojun Zhu [a], Peng Dai [b], Xinyu Lu [a], Haoquan Guo [a], Han Que [a], Dandan Wang [a], Tao He [a], Chaozhong Xu [a], Hossain Mahmud Robin [a], Zhenyang Luo [b,**], Xiaoli Gu [a,*]

[a] Co-Innovation Center for Efficient Processing and Utilization of Forest Products, College of Chemical Engineering, Nanjing Forestry University, Nanjing, 210037, China
[b] College of Science, Nanjing Forestry University, Nanjing, 210037, China

HIGHLIGHTS

- A renewable and eco-friendly lignin-based flame retardant was prepared.
- The flame retardant had better smoke suppression effect.
- A flame retardant mechanism of a lignin-based flame retardant was proposed.

GRAPHICAL ABSTRACT

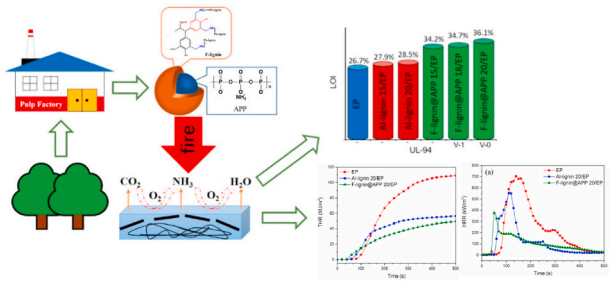

ARTICLE INFO

Keywords:
Lignin
Flame retardant
Epoxy resin
Smoke suppression

ABSTRACT

A renewable and eco-friendly lignin-based flame retardant was prepared to improve the flame retardant performance of epoxy resin (EP) by green and convenient one-step reaction of Ammonium Polyphosphate (APP), Melamine (MEL) and Al-lignin. Thermal and flame retardant properties test results showed that the properties of epoxy resin were significantly improved after adding 20% of flame retardant. Its carbon residue increased by 15.3 wt % and limit oxygen index value increased from 26.7% to 36.1%. In addition, it also showed excellent smoke suppression effect and low heat release rate. Its total smoke production (TSP) was 9.9 m^2 and total heat release (THR) rate was 53.1 MJ/m^2. In contrast, the TSP and THR of EP were much higher than 9.9 m^2 and 53.1 MJ/m^2, respectively. Kinetic analysis showed that the conversion rate ranging from 0.05 to 0.85 corresponded to activation energy between 97.83 kJ mol^{-1} and 327.45 kJ mol^{-1}. Flame retardant mechanism showed that the performance of this renewable and eco-friendly lignin-based flame retardant was excellent in fire suppression and smoke suppression.

1. Introduction

Epoxy resin (EP) is widely used in life, such as insulating materials used in electronic devices, semiconductor device plastic packaging, automotive adhesives, building decoration, etc [1–4]. There are many types of EP, among which the largest output and the most complete

* Corresponding author.
** Corresponding author.
E-mail addresses: luozhenyang@njfu.edu.cn (Z. Luo), guxiaoli@njfu.edu.cn (X. Gu).

https://doi.org/10.1016/j.matchemphys.2020.124101
Received 22 September 2020; Received in revised form 9 November 2020; Accepted 23 November 2020
Available online 26 November 2020
0254-0584/© 2020 Elsevier B.V. All rights reserved.

Table 1
The amounts and yield of the compounds in each reaction.

Reaction	Reactant	compounds	Yield
Step 2.2	20 g Al-lignin 18 g phenol	Ph-lignin: 19.74 g	51.95%
Step 2.3	6 g APP 5 g MEL	MELAPP: 8.43 g	76.63%
Step 2.4	4 g Ph-lignin 20 g MELAPP 7.2 g formaldehyde	F-lignin@APP: 27.1 g	86.86%

variety are bisphenol A epoxy resins. It accounts for more than 90% of the EP market share [5]. Although EP has excellent properties such as easy curing and work, good mechanical properties, good heat resistance and solvent resistance, its flammability has seriously affected its use in life. The limiting oxygen index (LOI) of epoxy resin is about 26%, which means it was flammable [6]. Therefore, it is very important to improve the flame retardant performance of epoxy resin.

Traditional halogen flame retardants have excellent flame retardant effect, they are often added to EP to improve the flame retardant performance of EP. Although halogen flame retardants can improve the flame retardant properties of EP, they will produce corrosive gases and black smoke when burned. These gases and black smoke are harmful for the environment and human health [7]. In recent decades, it has been found that intumescent flame retardants can be added to polymers as a substitute for halogen flame retardants. Such as Ammonium Polyphosphate (APP), APP has the functions of acid source and gas source, and has high content of phosphorus and nitrogen, good thermal stability, low smoke, and nontoxicity. It is one of the hotspots in the field of inorganic phosphorus flame retardants [8–10]. Compared with traditional flame retardants, intumescent flame retardants have the characteristics of eco-friendly, good flame retardant effect, high carbon residue, etc. The intumescent flame retardant is mainly composed of carbon source, acid source and gas source [11]. The carbon source is mainly some polyhydroxy compounds containing a large amount of carbon elements, such as pentaerythritol, ethylene glycol, etc. In recent years, with continuous research on biomass resources, it has been found that chitosan and lignin can replace pentaerythritol as a carbon source [12–15].

Lignin is the most abundant polymer in nature except cellulose [16,17]. It is one of the important components of the cell wall of woody plants [18,19]. The pulp produces large amounts of by-products containing lignin every year. This provides a basis for lignin to be used in a large number of industries. Lignin is a biopolymer with a three-dimensional network structure formed by three kinds of phenylpropane units connected to each other through ether bonds and carbon-carbon bonds. It is rich in aromatic ring structures, aliphatic and aromatic hydroxyl groups, and active groups such as quinone groups [20]. The special chemical structure of lignin gives it some other functions, and it can be added to plasticizers, solubilizers, stabilizers, flame retardants, surfactants, etc. In recent years, using lignin to prepare bio-based flame retardants has received widespread attention because of

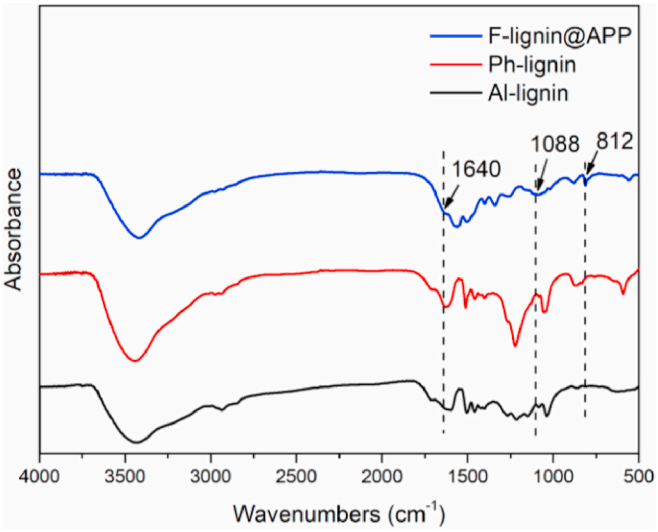

Fig. 2. FT-IR spectra of Al-lignin, Ph-lignin and F-lignin@APP.

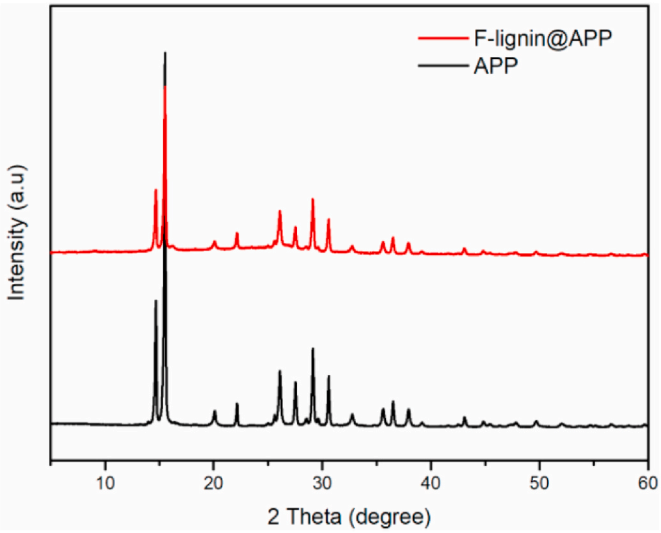

Fig. 3. Wide-angle XRD patterns of APP and F-lignin@APP.

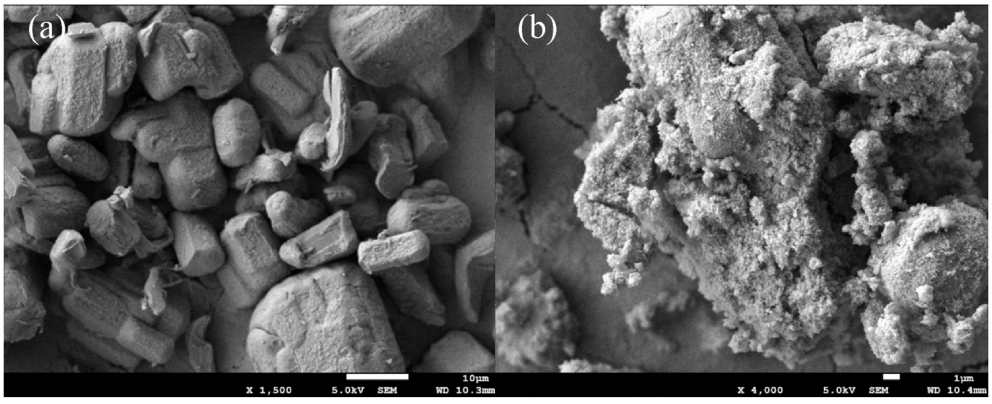

Fig. 1. SEM images of APP (a) and F-lignin@APP (b).

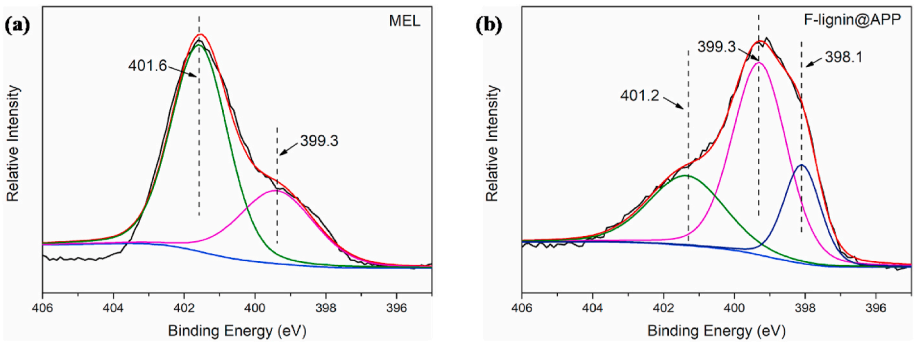

Fig. 4. N_{1s} spectra of MEL(a) and F-lignin@APP(b).

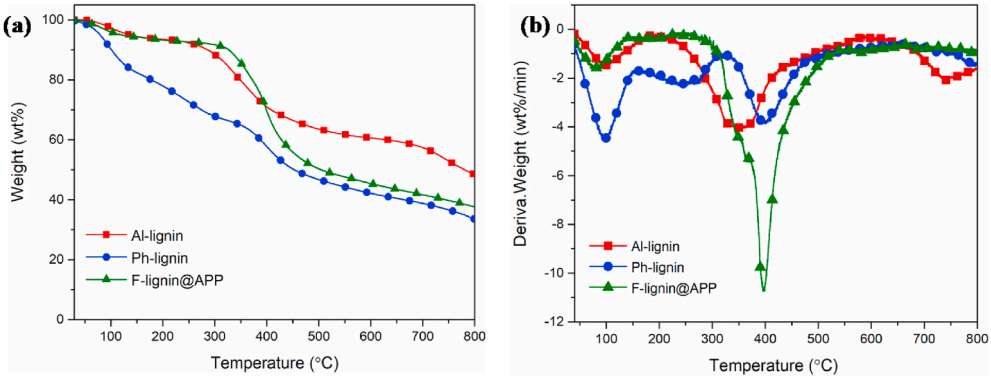

Fig. 5. TG (a) and DTG (b) curves of Al-lignin, Ph-lignin and F-lignin@APP.

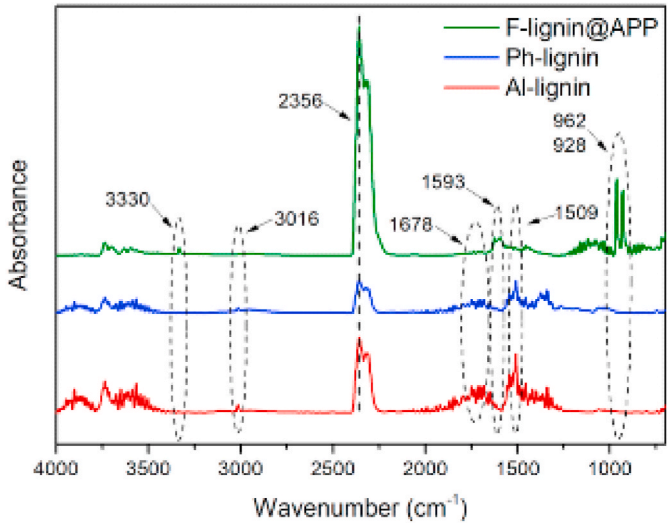

Fig. 6. FT-IR spectra of the volatile products of Al-lignin, Ph-lignin and F-lignin@APP.

the high carbon yield after decomposition of the aromatic framework of lignin. According to reports, about 35–40% of carbon can be produced after pyrolysis of lignin [21]. Taking advantage of this feature, proper addition of lignin to polymers (such as polypropylene, PBS, PET, etc.) can effectively reduce its flammability [22]. In addition, lignin has antioxidant properties and can be added to the polymer as a stabilizer to prevent aging of the polymer. In the past two decades, there have been some reports on lignin-based flame retardants. Some of them are about the modified lignin which grafted with some elements containing flame retardant effects such as P and N [23–26], and the flame retardancy of material improves a lot. Others are compounded with flame retardants.

Table 2
FTIR analysis of Al-lignin, Ph-lignin and F-lignin@APP [43].

Wavenumber/cm^{-1}	Functional groups	Vibrations
3330	N–H	Stretching
3016	C–H	Stretching
2356	C=O	Stretching
1593	C=N	Stretching
1509	Ph-H	Stretching
1100	P–O–C	Stretching
962	P–O-Ph	Stretching
928	P–O–P	Stretching

In the alkaline pulping process, the waste liquid is difficult to treat, and the by-product alkali lignin has not been fully utilized which mainly due to the high content of methoxy groups and the low content of hydroxyl groups (including phenolic hydroxyl groups and drunk hydroxyl groups). Alkali lignin contains a lot of syringyl, but the content of guaiacyl is less, resulting in lower chemical reaction activity [27]. Therefore, it is essential to find a way to utilize alkali lignin as much as possible.

In this article, the aim of the research is to prepare a flame retardant for EP which is simple to synthesize by using APP, Al-lignin and Melamine. With adding APP, not only improve the flame retardancy of EP, but also increase its smoke suppression. In this work, in order to prepare the lignin-based flame retardant, the alkali lignin was modified to increase its reaction site. Then, the lignin modified by phenolization is aminated and coated with APP. Before adding to EP, detailed characterization of its morphology and structure was carried out. After being added to EP, the flame retardant properties was evaluated obviously and its pyrolysis kinetics was studied.

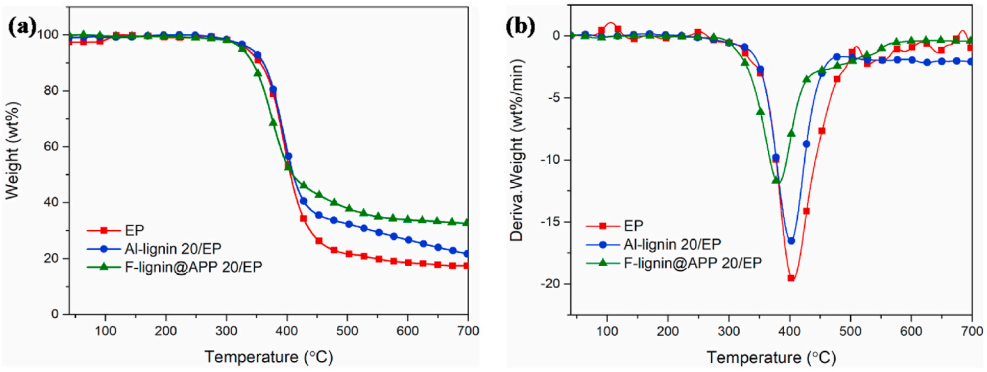

Fig. 7. TG (a) and DTG (b) curves of EP, Al-lignin20/EP and F-lignin@APP20/EP.

Table 3
TGA data of EP, Al-lignin20/EP and F-lignin@APP20/EP in N_2 atmosphere.

Samples	$T_{d5\%}$ (°C)	T_{dmax} (°C)	dW/dT (%/min)	residues (wt%)
EP	333	405	19.8	17.2
Al-lignin 20/EP	340	401	16.5	21.5
F-lignin@APP 20/EP	325	382	11.8	32.5

2. Experimental

2.1. Materials

Alkaline lignin (Al-lignin) was purchased from TCI Shanghai Co., Ltd.,China. Ammonium Polyphosphate (APP), 4,4-diaminodiphenylmethane (DDM) were provided by Shanghai Macklin Co., Ltd., China. Melamine (MEL) were offered by Shanghai Lingfeng Co., Ltd., China. Formaldehyde, N,N-diemthylformamide (DMF), diethyl ether and ethanol were purchased from Nanjing Chemical Reagent Co., Ltd., China. The amounts and yield of the compounds in each reaction was shown in Table 1.

2.2. Phenolization of alkaline lignin (Ph-lignin) [28–30]

First, 20 g Al-lignin was added to a flask containing 80 ml H_2SO_4 (2 mol/L) solution and heated up to 80 °C and stirred for 1.5 h. Then, when the temperature was raised to 95 °C, 18 g phenol (0.2 mol) was added, and the mixture was stirred at reflux for 1.5 h. After the reaction completed, the mixture was washed three times with 500 ml of diethyl ether and dried at 70 °C overnight to a constant weight.

2.3. Preparation of MEL and APP mixture (MELAPP)

6 g APP (mass ratio, APP: MEL = 1.2:1) was added to 140 ml ethanol in water (mass ratio, ethanol: water = 5:2) and stirred for 30 min, allowed the APP to be fully dispersed in the solution. Then 5 g MEL (0.04 mol) was added, temperature was raised to 70 °C and stirred for 6 h. After completion, the mixture was cooled to room temperature, washed repeatedly with ethanol for 3 times, and then dried at 70 °C for 12 h.

2.4. Preparation of lignin-based flame retardant (F-lignin@APP)

4 g phenolated lignin and 20 g MELAPP (mass ratio, Ph-lignin: MELAPP = 1:5) were added to a flask with 250 ml DMF, then 7.2 g (0.24 mol) of formaldehyde was added at 75 °C, and stirred under reflux for 3 h. After the reaction was completed, 500 ml of distilled water was added, and the solid was filtered. It was washed three times with 500 ml of distilled water, dried at 70 °C under vacuum for 24 h.

2.5. Preparation of flame retardant EP composites (F-lignin@APP20/EP)

3 g F-lignin@APP and 15 g of EP were mechanically stirred for 1.5 h and 700 rpm to make the mixture uniform. After stirring, 3 g DDM (mass ratio, DDM: EP = 1:5) was added and stirred for 1.5 h. Then the bubbles were removed in vacuum oven and the uniformly mixed resin was poured into the mold, cured at 100 °C for 2 h, and elevated at 150 °C for 2 h.

2.6. Kinetic modeling

The decomposition process of lignin epoxy resin composite material is a solid state reaction process [31,32]. Generally, the decomposition rate can be expressed by the parametric equation of $f(\alpha)$ and $K(T)$, which is as follows:

$$\frac{d\alpha}{dt} = \beta\frac{d\alpha}{dT} = K(T)f(\alpha)h(P) \quad (1)$$

where α is the conversion rate (%) of the sample in the reaction temperature range, β is the linear heating rate (°C/min), T is the reaction temperature (K), and P is the pressure (Pa). Although pressure may have an impact on kinetic analysis, pressure is usually ignored in pyrolysis kinetic analysis of solid state reactions because the supplied gas flows remain constant in the experiments [33,34]. After ignoring the pressure, Eq. (1) can be written as a function containing two variables (α and T):

Table 4
Flame retardant of EP, Al-lignin 20/EP and F-lignin@APP 20/EP.

Sample	EP (wt%)	DDM (wt%)	Al-lignin (wt%)	F-lignin@APP (wt%)	LOI (%)	**UL-94 rating**
EP	83.3	16.7	–	–	26.7	–
Al-lignin 15/EP	70.8	14.2	15	–	27.9	–
Al-lignin 20/EP	67.7	13.3	20	–	28.5	–
F-lignin@APP 15/EP	70.8	14.2	–	15	34.2	–
F-lignin@APP 18/EP	68.3	13.7	–	18	34.7	V1
F-lignin@APP 20/EP	67.7	13.3	–	20	36.1	V0

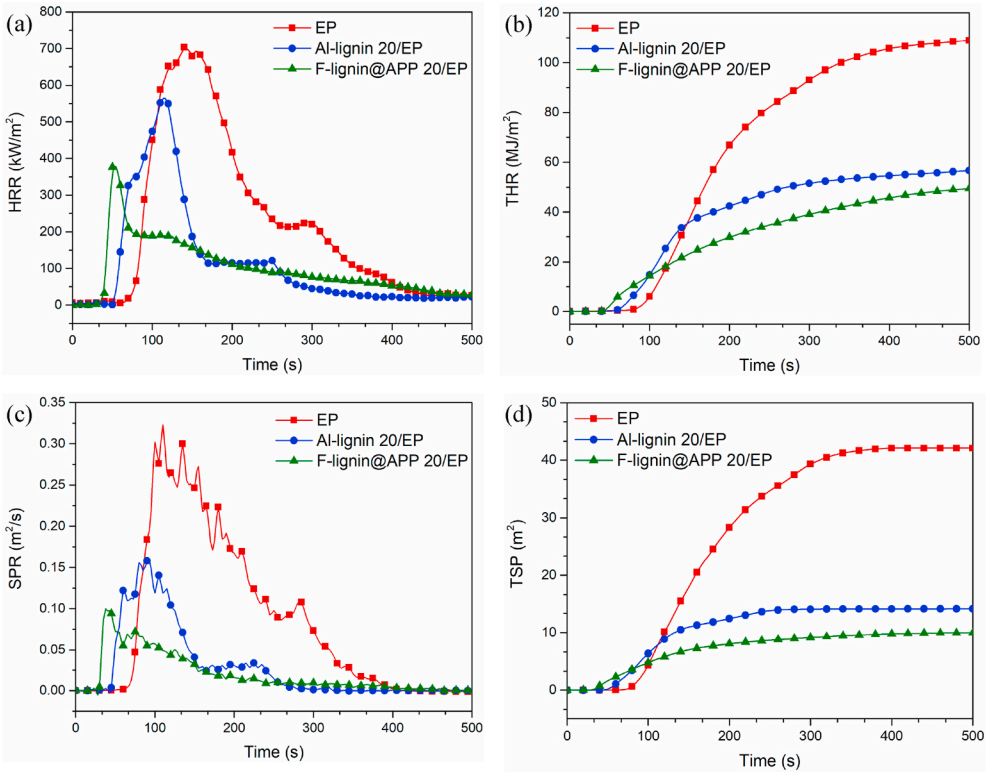

Fig. 8. HRR (a), THR (b), SPR (c) and TSP (d) curves of EP, Al-lignin 20/EP and F-lignin@APP 20/EP.

Table 5
Detailed data obtained from cone calorimeter tests of EP, Al-lignin 20/EP and F-lignin@APP20/EP.

sample	EP	Al-lignin 20/EP	F-lignin@APP20/EP
TTI (s)	60 ± 3	44 ± 2	31 ± 2
THR (MJ/m^2)	108.9 ± 2.1	57.5 ± 1.9	53.1 ± 1.9
PHRR (kW/m^2)	703.6 ± 10.3	571 ± 7.6	385.4 ± 8.0
TSP (m^2)	42 ± 2.9	14.1 ± 3.1	9.9 ± 2.6
Peak SPR (m^2/s)	0.32 ± 0.03	0.16 ± 0.02	0.09 ± 0.02
Average MLR (g/s)	0.101 ± 0.011	0.066 ± 0.009	0.049 ± 0.005
Residue (wt%)	5.3 ± 0.7	16.6 ± 1.1	25.5 ± 1.6

$$\frac{d\alpha}{dt} = \beta\frac{d\alpha}{dT} = K(T)f(\alpha) \tag{2}$$

The conversion rate (α) can be obtained by Eq. (3):

$$\alpha = (M_0 - M_T) / (M_0 - M_\infty) \tag{3}$$

where M_0 is the initial mass of the sample, M_T is the mass of the sample residue at the corresponding temperature, M_∞ is the mass of the sample residue at the final temperature. The temperature-dependent equation $K(T)$ is derived from the Arrhenius equation:

$$K(T) = A\exp(-E/RT) \tag{4}$$

where A and E are kinetic parameters. A is pre-exponential factor, E is apparent activation energy (kJ/mol) and R is gas constant (8.314 J/(mol·K)).

Bring Eq. (4) into Eq. (2), separate the variables, and integrate the equation to get Eq. (5):

$$G(\alpha) = \int_0^\alpha d\alpha / f(x) = \frac{A}{B}\int_0^T exp(-E/RT)dT = (AE/\beta R)P(u) \tag{5}$$

where $G(\alpha)$ is the integral form of $f(x)$, u is usually defined as the temperature integral of E/RT and $P(u)$. $P(u)$ has many mathematical assumptions to determine the activation energy.

In the absence of a kinetic model, there are several ways to obtain the activation energy during the reaction. Usually these methods are divided into differential method and integral method. Integral method usually deviates greatly from the actual value. Compared with integral method, differential method does not involve approximate values, so the results obtained are more accurate.

Kissinger Akahira-Sunoe (KAS) and Flynn-Wall-Ozawa (FWO) are two methods commonly used to obtain the activation energy of thermal decomposition:

$$\ln(\beta / T^2) = \ln(AR / EG(\alpha)) - E / RT \tag{6}$$

$$\ln(\beta) = \ln(AR / EG(\alpha)) - 2.315 - 0.4567E / RT \tag{7}$$

Through these two methods, the value of the activation energy (E) can be obtained from the slopes of $\ln(\beta/T^2)$ vs $1/T$ or $\ln(\beta)$ vs $1/T$.

2.7. Measurements

Fourier transform infrared (FTIR) spectra were recorded by a Nicolet 6700 FTIR spectrometer under the resolution of 1 cm^{-1} in 32 scans by a KBr disk with the wavenumber ranging from 4000 to 500 cm^{-1}. Thermogravimetric analysis (TGA) was obtained on DTG-60AH (SHIMADZU, Japan). The epoxy resin composites (about 5 mg) were heated from 30 to 700 °C at a rate of 15 °C min^{-1} under the nitrogen flow of 40 ml min^{-1}. The X-ray photoelectron spectroscopy (XPS) spectra were recorded by an AXIS UltraDLD spectrometer with Al Kα (1486.6eV) radiation. The surface morphologies of the sample were observed by using a JEOLJSM-7600 scanning electron microscopy (SEM) (JEOL, Japan) at the accelerating voltage of 15 kV. Limiting oxygen index (LOI) values were measured using a HC-2C oxygen index meter (Jiangsu Institute of Chemical Industry, China) and the size of three samples was 100 mm × 10 mm × 3 mm according to ASTM D2863-97. Vertical burning (UL-94) was conducted on a CZF-2 instrument (Jiangsu Institute of Chemical Industry, China) and the size of three epoxy resin composites was 100

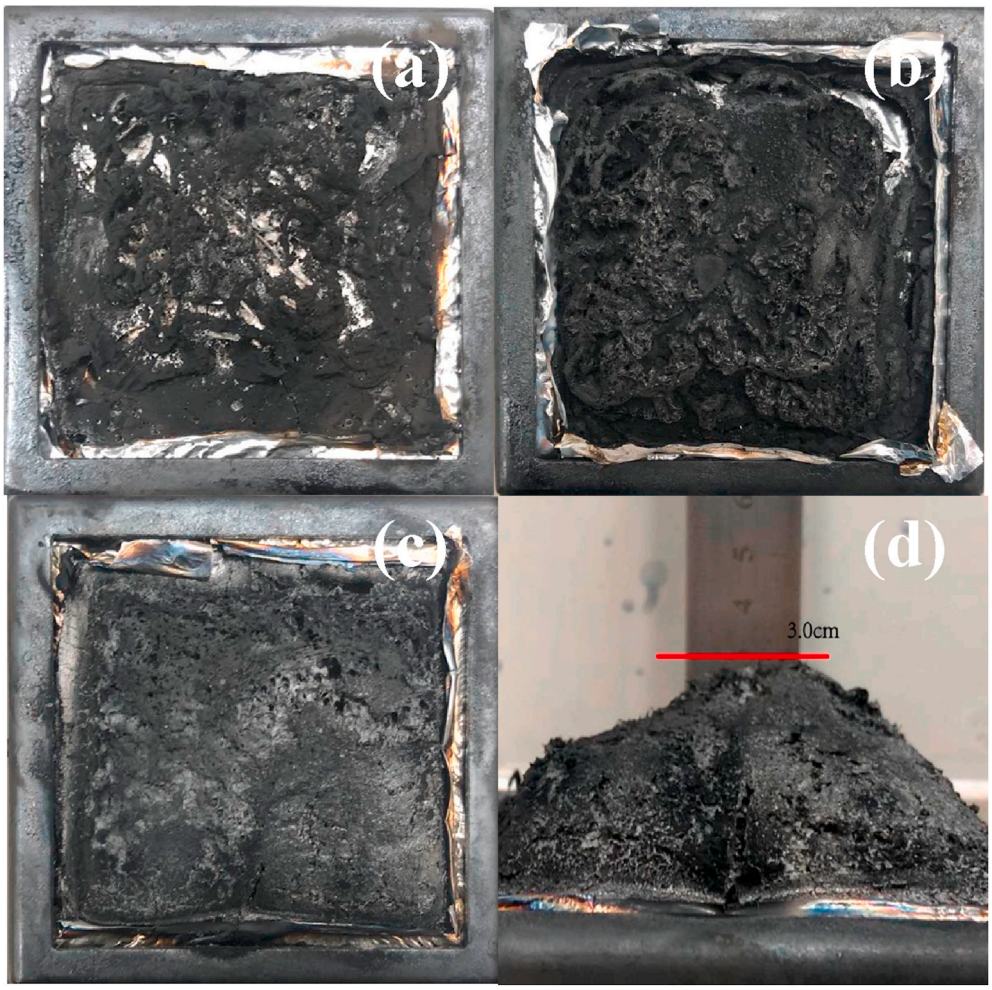

Fig. 9. Digital pictures of the residues of EP (a), Al-lignin 20/EP (b) and F-lignin@APP20/EP (c,d) after cone calorimetry tests.

mm × 10 mm × 3 mm according to ATSM D3801 standard. Combustion behavior of the samples were measured by cone calorimeter (Fire Testing Technology, UK). The samples for each formulation with dimension of 100 mm × 100 mm × 3.2 mm were exposed to a radiant cone at a heat flux of 50 kW/m^2 according to ISO 5660. The samples were backed with aluminum foil in a metal frame. Laser Raman spectroscopy (LRS) is to test the residue by configuring a laser system with a wavelength of 532 nm. The TG-FTIR analysis was conducted on a thermogravimetric analysis (TGA, Perkin Elmer Pyris 1 TGA unit), coupled with a Fourier transform infrared spectrometry.

3. Results and discussion

3.1. Characterization of F-lignin@APP

Through SEM, the morphology of APP and F-lignin@APP can be observed clearly. As shown in Fig. 1, there are obvious differences between APP and F-lignin@APP. The surface of APP is smooth without fine particles. After being coated with F-lignin, there are many small particles appearing on the surface of APP, and the size of these particles is about 1 μm. This indicates that F-lignin can be used to coat APP through the Mannich reaction.

The FT-IR spectra of Al-lignin, Ph-lignin, F-lignin@APP are shown in Fig. 2. From Fig. 2, it shows that the basic structure of lignin does not change much after phenolation. Aromatic skeletal stretching vibrations shift from 1600 cm^{-1} and 1503 cm^{-1} to 1624 cm^{-1} and 1512 cm^{-1}, C–H bending and out-of-plane deform vibrations shift from 1460 cm^{-1} and 858 cm^{-1} to 1458 cm^{-1} and 873 cm^{-1} [35]. The peak at 1222 cm^{-1} is assigned to syringyl structure. Its absorption peak intensity increases, indicating that the phenolization of lignin was successful [36]. After F-lignin@APP wrapped APP, some absorption peaks appeared, such as the absorption peak of N–H bending vibration in NH_2 structure at 1640 cm^{-1}, the absorption peak of the triazine ring at 813 cm^{-1}, and the absorption peak of the stretching vibration P–O at 1088 cm^{-1} [37]. The results show that Al-lignin is phenolized and the APP is successfully introduced into F-lignin.

XRD is an effective characterization method of studying the crystal form changes of materials. Fig. 3 is the wide-angle XRD spectra of APP and F-lignin, as seen from the curve of APP, there is a broad peak over the range of 15–30°, indicating its amorphous structure [38]. Meanwhile, the two curves reveal that APP and F-lignin @ APP have the same diffraction peaks. This means that the process of preparing lignin-based flame retardant did not change the crystalline of APP.

The chemical composition and types of chemical bonds can be analyzed by XPS spectra. The N_{1s} spectra of MEL and F-lignin@APP are shown in Fig. 4. It can be seen from Fig. 4(a) that the peak at 401.6 eV represents NH_2 in MEL and the peak at 399.3 eV may stand for the nitrogen in the C=N double bonds of MEL [39]. As can be observed from Fig. 4(b), the peak of C]N double bond in F-lignin@APP still appears at 399.3 eV and the intensity of the C=N peak is much higher than MEL. After functionalization, two new peaks appeared, the peak at 401.2 eV corresponds to NH_4^+ in APP. Another peak at 398.1eV should be attributed to the N in the –NH– for F-lignin@APP [40]. The findings clearly manifest that MEL and APP are successfully introduced to F-lignin.

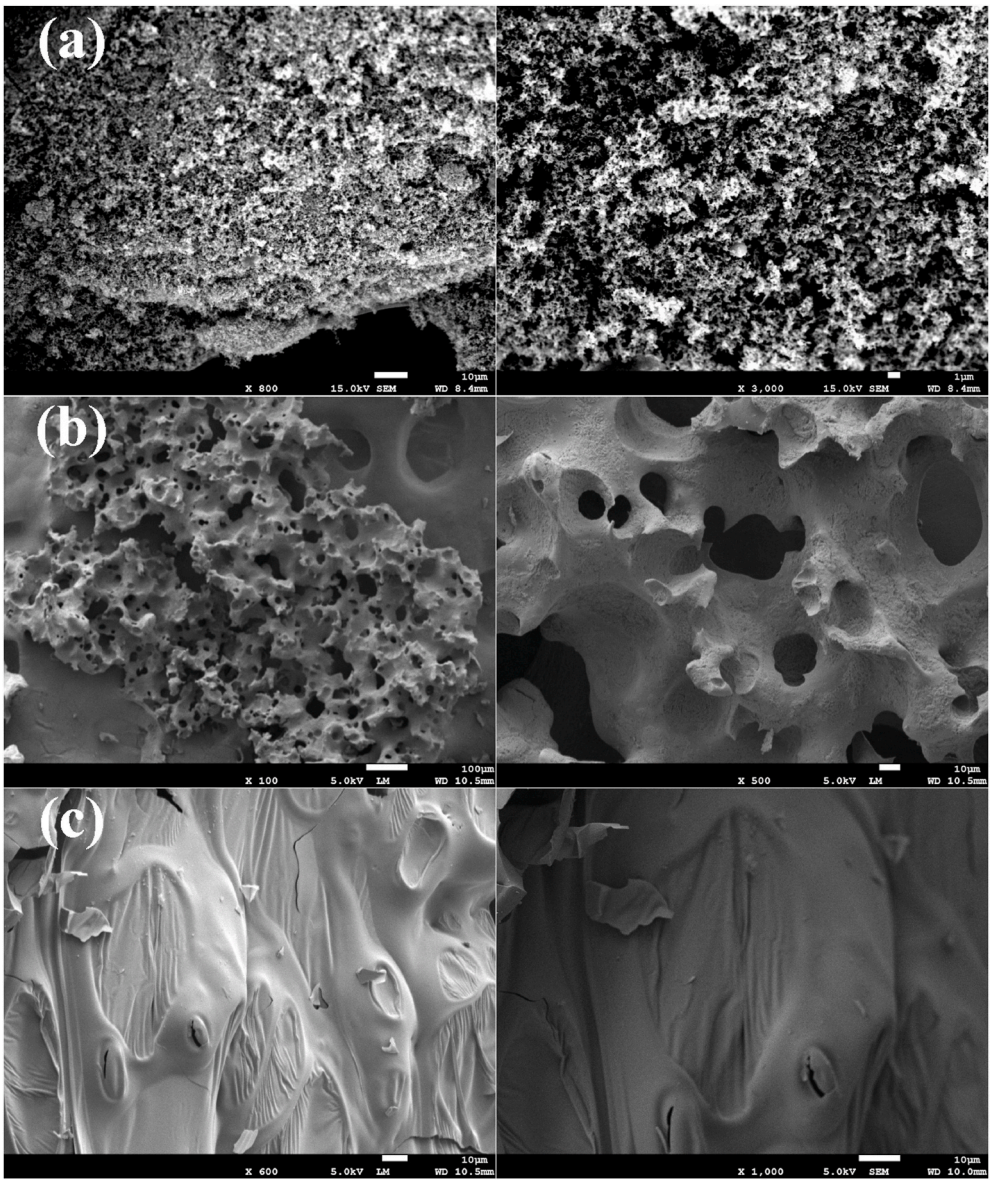

Fig. 10. SEM images of EP (a), Al-lignin 20/EP (b) and F-lignin@APP20/EP (c).

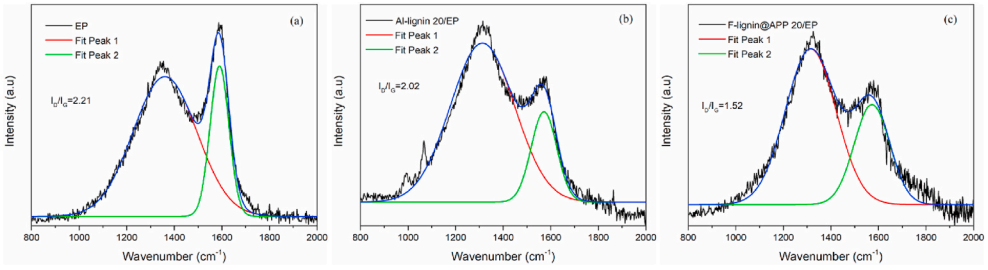

Fig. 11. LRS spectra of the residues of EP (a), Al-lignin 20/EP (b), F-lignin@APP 20/EP (c).

The TG and DTG curves in N_2 atmosphere of Al-lignin, Ph-lignin and F-lignin@APP are shown in Fig. 5. As can be observed from Fig. 5(a), the carbon residues of Ph-lignin and F-lignin@APP are reduced compared with Al-lignin, which are 33.5% and 37.5%, respectively. In the curve of F-lignin@APP, it can be seen that the second weight drop is sharp and mainly associates with the release of phosphoric acid, polyphosphoric acid, and metaphosphoric acid within APP decomposition when subjected to elevated temperature up to 800 °C [41]. From Fig. 5(b), the DTG curves o-f three samples all show a peak before 150 °C, which is caused by the evaporation of the residual moisture contained in three samples. Unlike Al-lignin and F-lignin@APP, Ph-lignin have a broad endothermic peak at 160–320 °C. This broad peak is formed by the decomposition and volatilization of lignin with lower molecular weight. At 320–500 °C, Al-lignin, Ph-lignin and F-lignin@APP all have an

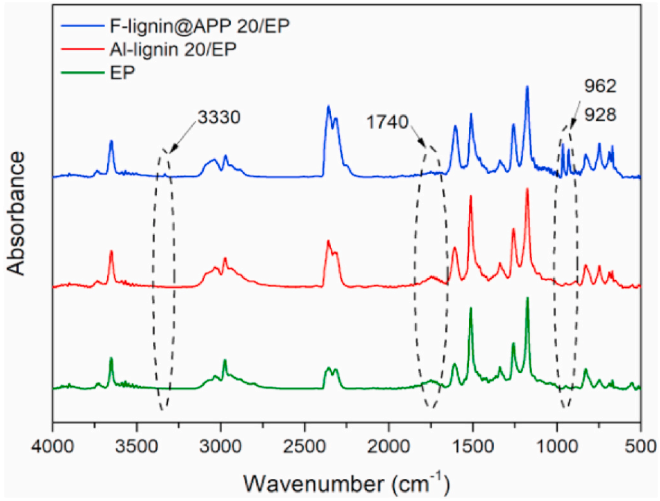

Fig. 12. FT-IR spectra of the volatile products of EP, Al-lignin20/EP and F-lignin@APP20/EP.

endothermic peak. It is because the bonds between structural units of lignin were broken and some monomer phenols evaporated. In addition, it can be found that the endothermic peak of F-lignin@APP is much stronger than the other two peaks. It is due to not only the degradation of lignin but also the decomposition of APP during the heating process. The APP used in the experiment was APP II, its decomposition temperature was about 400 °C, so it is consistent with TG results [42]. The results show that the APP is successfully introduced into F-lignin. Combining SEM, FTIR, XRD, XPS test results, it can be considered that F-lignin successfully wrapped the APP.

FT-IR of the volatile products of Al-lignin, Ph-lignin and F-lignin@APP are shown in Fig. 6. Table 2 listed peak ranges, functional groups and vibration types. It is nothing that the characteristic peaks of F-lignin@APP are 3330, 2356, 1593, 1509, 1100, 962 and 928 cm^{-1}. Among them, the peaks at 3330 $cm^{-1}$and 1593 cm^{-1} are the absorption peaks of N–H and C]N. The peaks at 1100, 962 and 928 cm^{-1} illustrate the presence of phosphoric acid derivatives, which are attributed to P–O–C, P–O-Ph, P–O–P, respectively [43]. Compared with Ph-lignin and Al-lignin, the absorption peaks of F-lignin@APP do not contain hydrocarbon compounds, carbonyl compounds and aromatic compounds. These compounds are usually formed by breaking the chemical bonds of functional groups on the basic structural units of lignin. It illustrates that the depolymerization products of lignin synergized with the polyacid generated by APP decomposition to form phosphorus-containing derivatives [44]. Then, the absorption peaks of these compounds in the volatile products disappeared.

3.2. Thermal and fire properties of F-lignin@APP20/EP

Fig. 7 shows the degradation process of EP, Al-lignin 20/EP and F-lignin@APP20/EP under N_2 atmosphere, and the detailed data are listed in Table 3. As for DTG curves shown in Fig. 7, there is a classic one-step decomposition peak represented under nitrogen atmosphere [45]. From Table 3, the T_{dmax} (the temperature where the maximum decomposition rate) of EP, Al-lignin 20/EP and F-lignin@APP20/EP are 405 °C, 401 °C and 382 °C, respectively. This phenomenon was explained as follows. On the one hand, because of the presence of APP in flame retardant and the decomposition temperature of APP is low; on the other hand, excessive curing agents in the matrix resulted in early weight loss. The maximum decomposition rate of F-lignin@APP20/EP is 11.8%/min, which is 8%/min and 4.7%/min lower than EP and Al-lignin. Since the carbon in EP cannot form carbon dioxide in a nitrogen atmosphere, the char residue of EP is 17.2 wt%. However, the char residue of F-lignin@APP20/EP is as high as 32.5 wt%. It is much higher than EP which almost 2 times to EP reference. The high char residue, beyond doubt, is beneficial to flame-retardant effects, especially in the condensed phase.

In order to investigate the flame retardance of the EPs, the LOI tests and vertical burning tests (UL-94) were carried out at the room temperature and the results are showed in Table 4. From Table 4, it is easy to observe that as the content of Al-lignin or the F-lignin@APP increases, the LOI of the EP increases. With adding the Al-lignin, the LOI of EP just increases a little so that the rating hard to reach V-1 or V-0. However, with the F-lignin@APP adding, the LOI exceeds 30% while the content

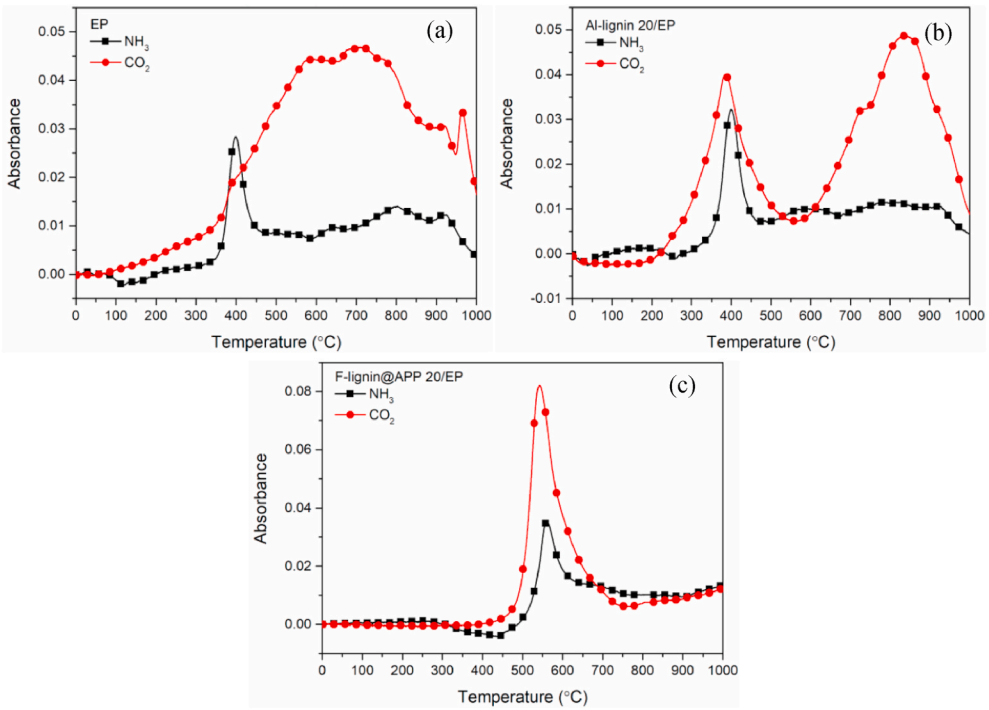

Fig. 13. The evolution of CO_2 and NH_3 of EP (a), Al-lignin20/EP (b) and F-lignin@APP20/EP (c) during the heating process.

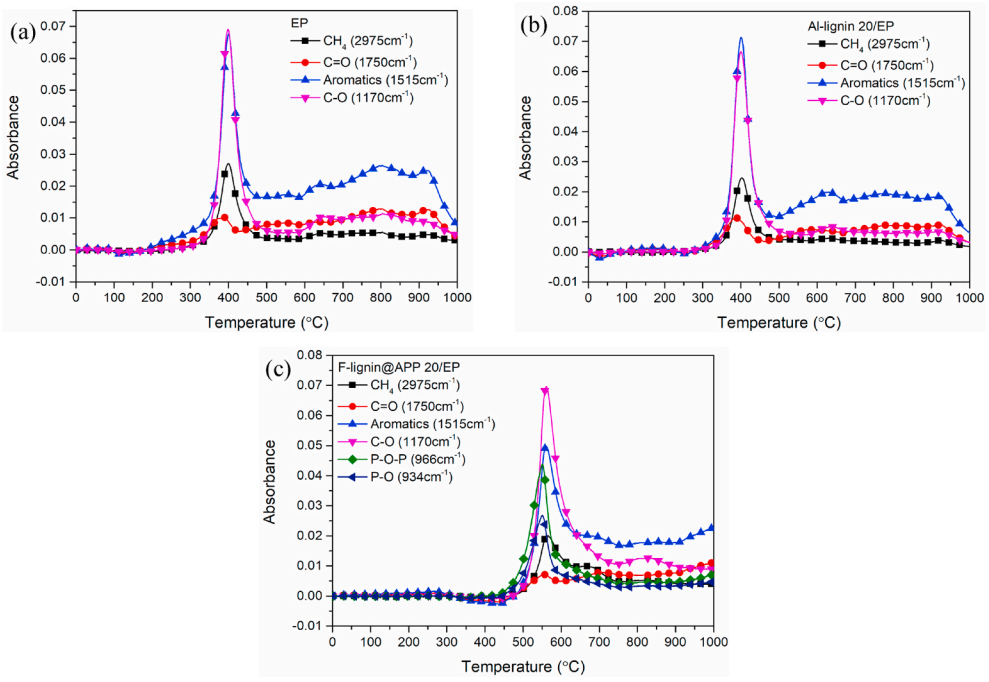

Fig. 14. The evolution of other volatiles of EP (a), Al-lignin 20/EP (b) and F-lignin@APP20/EP (c) during the heating process.

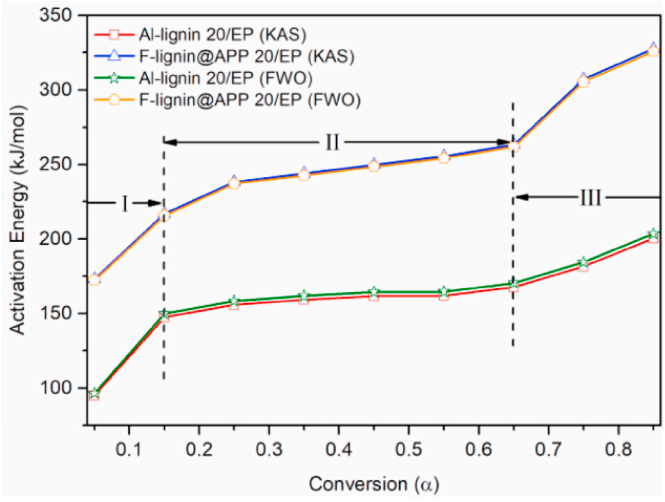

Fig. 15. Activation energy of Al-lignin 20/EP and F-lignin@APP20/EP at different conversion rates.

of F-lignin@APP is 15 wt%. As the content of F-lignin@APP increases, the LOI of EP reaches to 34.7% and a V-1 classification at the thickness of 3 mm. While the content of F-lignin@APP reaches to 20 wt%, the result of the LOI test indicates that the F-lignin@APP20/EP gets a LOI (36.1%) which is much higher than LOI of EP. Moreover, it is easy to reach a V-0 classification with 20 wt% of the F-lignin@APP is added.

Cone calorimetry was an effective test method to research the burning behavior of a material. Variety of parameters, including the heat release rate (HRR), the total heat release (THR), the smoke production rate (SPR) and the total smoke production (TSP) curves of EP, Al-lignin 20/EP and F-lignin@APP20/EP are shown in Fig. 8, and the data are presented in Table 5. The error of our samples is within 3%. From Fig. 8, the PHRR of EP is 703.6 kW/m^2. After adding Al-lignin and F-lignin@APP respectively, the PHRR of Al-lignin 20/EP and F-lignin@APP20/EP reduce obviously, they are 571 kW/m^2 and 385.4 kW/m^2 respectively. Generally, a much lower PHRR of material indicates that the flame retardant can reduce heat hazard when burned. Moreover, compared with EP, Al-lignin 20/EP and F-lignin@APP20/EP have lower THR. The THR of F-lignin@APP20/EP (53.1 kW/m^2) is only about half as much as EP (108.9 kW/m^2) which is in accordance with the results of PHRR. The result indicates that F-lignin@APP can reduce the heat release rate of EP during combustion, thus achieving some flame-retardant effects. In addition, TTI value of EP is higher than F-lignin@APP20/EP, the reason for the phenomenon may be the degradation products of F-lignin@APP such as phosphoric and poly-/pyro-phosphoric acids can induce the dehydration and further decomposition of EP [46]. What's more, the residues of Al-lignin 20/EP and F-lignin@APP20/EP increase a lot after the combustion and far more than the residues of EP. This suggests that Al-lignin and F-lignin@APP can not only reduce the exothermic rate but also increase the amount of residue.

3.3. Characterization of condensed phase

The digital graphs of char residues of EP, Al-lignin and F-lignin after the cone calorimetry test are shown in Fig. 9. From Fig. 9 it shows that EP and Al-lignin 20/EP have less residue, and the residue appears sparse. Contrary to EP and Al-lignin, F-lignin@APP20/EP has more residues, dense structure and a certain expansion of the carbon layer.

Fig. 10 is the morphology of carbon residue after cone calorimetry observed by SEM. From Fig. 10, it is easy to find that the carbon layer of EP is sparse and messy. Although the carbon layer of Al-lignin is continuous, it has many holes. Compared to EP and Al-lignin20/EP, the carbon layer of F-lignin@APP20/EP appears to be continuous and dense. Such a carbon layer can block heat and flammable gases from entering the polymer, thereby improving the flame retardant properties of the polymer.

Raman I_D/I_G ratios were usually used to evaluate the quality of carbon materials, because it represented the degree of graphitization. G-band is related to the vibration of sp2-hybridized carbon atoms in the graphite layer and D-band is associated to vibration the carbon atom with dangling bonds at the flat end of the disordered graphite or glassy carbon [47]. From Fig. 11, the G-band and D-band are located nearly at 1328 cm^{-1} and 1578 cm^{-1} respectively. The I_D/I_G rate of EP is 2.21 and due to the presence of Al-lignin, the I_D/I_G rate of Al-lignin sharply

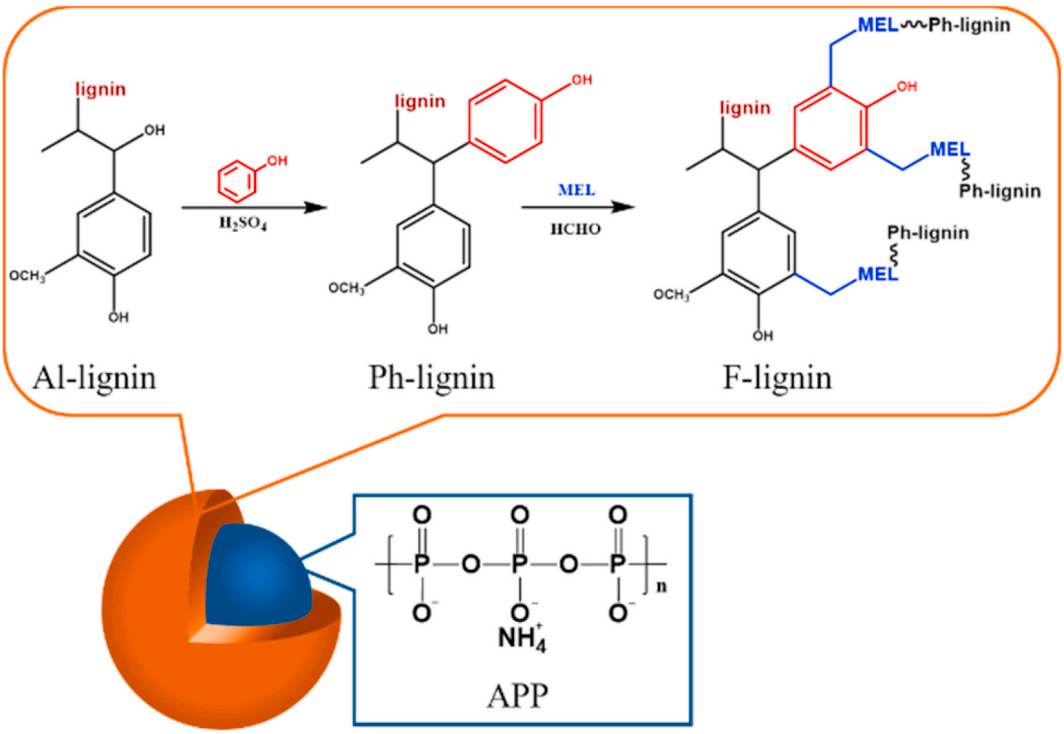

Scheme 1. The synthesis route of F-lignin@APP.

reduces to 2.02, indicating a higher graphitization degree. The value of F-lignin@APP20/EP is lower than that of Al-lignin 20/EP and reaches to 1.52, this means that the carbon it produces is more graphitized and ordered, higher degree of graphitization has certain benefits for flame retardancy [48].

3.4. Characterization of gas phase

Fig. 12 is FT-IR of the volatiles of EP, Al-lignin and F-lignin at T_{dmax}. From Fig. 12, the fact that they have several same absorption peaks can be observed. The peak near 3650 cm^{-1} is the absorption peak of NH_3 and H_2O. The peak at 2975 cm^{-1} is attributed to the stretching vibration absorption peak of hydrocarbon. The peak at 2358 cm^{-1} is assigned to the stretching vibration absorption peak of C]O in CO_2. The peak at 1750 cm^{-1} is the absorption peak of carbonyl component, and the peaks near 1515 cm^{-1} are the absorption peaks of aromatic component [49]. The peaks around 1170 cm^{-1} are mainly the absorption peaks of C–C and C–O in the structure of phenols and ethers. These absorption peaks are due to the epoxy resin used in the experiment is bisphenol A type and the use of amino group containing curing agent (DDM) generated, which is consistent with other researchers reported [50,51]. Unlike Al-lignin 20/EP and EP, F-lignin@APP20/EP has several new absorption peaks. The peak at 3330 cm^{-1} is the absorption peak of NH_2 in melamine. The peaks at 962 cm^{-1} and 928 cm^{-1} are the absorption peak of phosphorus-containing derivatives, they are P–O–P and P–O, respectively. In addition, the absorption peak intensity of carbonyl compound decreases. These phenomena indicate that F-lignin@APP20/EP can produce polyacids and NH_3 during pyrolysis. These polyacids interact with the carbon produced by the decomposition of lignin to form a condensed phase. This layer of condensed phase blocks some of the volatiles.

TG-FTIR can be used to study the evolution of gas-phase products of flame retardants. Based on the Lambert-Beer law, the change in absorption peak intensity represents the evolution of volatile concentration [51]. Fig. 13 shows the changing trend of CO_2 and NH_3 in each samples with the temperature increase process. The tendency showed that CO_2 is continuously produced, during the heating process of EP. The CO_2 absorption peak intensity change rule of Al-lignin is M type. This is because lignin begins to depolymerize and some decarbonylation and decarboxylation reactions occur, resulting in an increase in the intensity of the absorption peak of CO_2 at lower temperature. As the temperature rises, the secondary decomposition of the depolymerized volatiles and the formation of new carbon are the main reason for the CO_2 enhancement at high temperatures. Compared with EP and Al-lignin, F-lignin has only a sharp CO_2 change peak, indicating that a large amount of CO_2 is produced at once at 550 °C. A large amount of non-combustible gas can dilute the combustible gas, so as to achieve the effect of suppressing combustion [52].

Fig. 14 shows the changing trend of hydrocarbons, aromatics, ethers and other compounds in each samples with the temperature increase process [52]. It is worth noting that the absorption peaks of various compounds of EP, Al-lignin 20/EP and F-lignin@APP20/EP are concentrated in 399, 400 and 556 °C, respectively. The main volatiles of EP are aromatic compounds and ether compounds. The main volatiles of EP are aromatic compounds and ether compounds. Al-lignin 20/EP has the same volatiles as EP, and their trends are similar. Since F-lignin@APP contains APP, there are some phosphorus derivatives in its volatile products. In addition, its absorption peak trend is also different from EP and Al-lignin 20/EP. The main volatiles of F-lignin@ APP 20/EP are ethers, aromatics and phosphorus compounds. Their absorption peak intensity is ethers > aromatics > P–O–P. In EP and Al-lignin 20/EP, the absorption peak intensity of aromatic compounds is similar to that of ether compounds. This is because phosphorus derivatives can promote the formation of carbon. Lignin can form a large amount of carbon mainly due to its aromatic structure. During pyrolysis, phosphorus derivatives can interact with lignin [53], thereby reducing the volatilization of aromatic compounds and forming a large amount of carbon residue.

3.5. Kinetics analysis

Fig. 15 shows the activation energy of Al-lignin 20/EP and F-

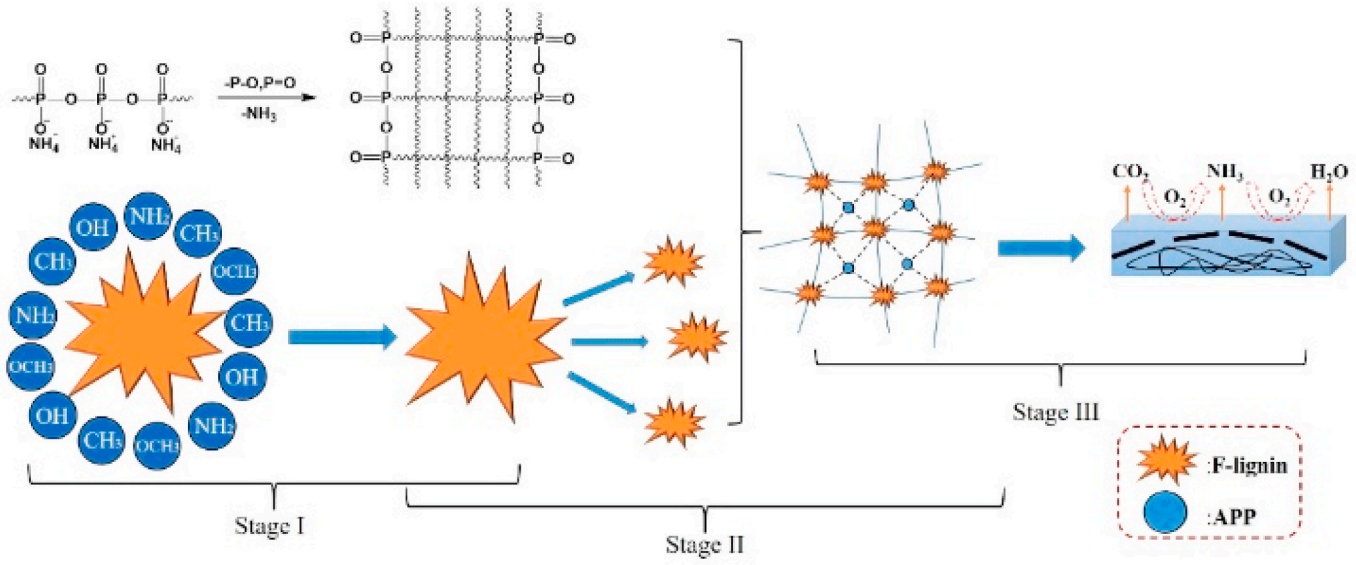

Scheme 2. The possible fire retardant mechanism of F-lignin@APP

lignin@APP20/EP at different conversion rates. It can be seen that whether it is added EP of Al-lignin or F-lignin@APP, its thermal decomposition is a very complicated process, which is accompanied by many reactions. Combined with gas phase analysis, the pyrolysis process of Al-lignin 20/EP and F-lignin@APP20/EP can be divided into three stages.

In stage I, the activation energy required for pyrolysis is low. At this stage, it is mainly the cleavage of hydroxyl, methyl, methoxy and other functional groups in lignin structure [54]. The activation energy required for the cleavage of these functional groups is low. Also, the APP in F-lignin@APP will decompose, producing some phosphorus-containing derivatives and NH_3 at this stage.

In stage II, lignin will depolymerize at higher temperature. The thermal stability of ether bond is lower than that of C–C bond, so this kind of bond will be broken first [55]. This leads to more ether compounds in volatiles. In addition, the decomposition products of APP will also interact with the depolymerization products of lignin at this stage. Therefore, the growth rate of the activation energy of F-lignin@APP20/EP is higher than that of Al-lignin 20/EP in Fig. 15.

In stage III, this is already in the late stage of pyrolysis. From Fig. 15, it is clear that the value and growth rate of activation energy of F-lignin@APP20/EP are much higher than that of Al-lignin 20/EP. This shows that the carbon layer formed by F-lignin@APP20/EP is more stable than Al-lignin 20/EP (see Scheme 1).

3.6. Flame retardant mechanism analysis

Based on the above analysis results, the flame retardant mechanism of F-lignin@APP is shown in Scheme 2. During stage I, the functional groups of F-lignin in F-lignin@APP would be broken and some gas would be generated. In addition, this stage was also accompanied by the decomposition of APP, producing NH_3 and polyacids. The flammable gas was diluted by the gas generated from decomposition, thereby slowing the combustion. At stage II, the aromatic ring skeleton structure of lignin began to break and interacted with polyacids. Then, as the polyacid continuously promoted the esterification and dehydration of decomposition products, new char residue gradually formed. At stage III, the newly formed carbon became a dense and strong carbon layer under the action of polyacids. The gas products produced caused the carbon layer to expand. A barrier was formed by a carbon layer between EP and heat source. Combustible gases were prevented by the barrier from entering EP, thereby the flame retardancy of F-lignin@APP was achieved.

4. Conclusions

In this work, a lignin-based flame retardant containing P and N (F-lignin@APP) was successfully prepared via wrapping APP with F-lignin which make EP perform excellent flame retardant properties. By comparing the flame retardancy of epoxy resins with Al-lignin and F-lignin@APP added respectively. It is concluded that the epoxy resin with Al-lignin does not show a good flame retardant because Al-lignin only serves as a carbon source. When F-lignin@APP is added into epoxy resin, the synergy of APP and F-lignin make EP perform good flame retardant properties. Fire properties test results show that F-lignin@APP can improve the LOI value of EP, and has better smoke suppression effect (9.9 m^2) and lower heat release rate (53.1 MJ/m^2). Kinetic analysis show that when the conversion rate is 85%, the corresponding activation energy was 327.45 kJ mol^{-1}. Through the analysis of its flame retardant mechanism, it can be found that the polyacid generated by the decomposition of APP will synergize with the carbon generated by the lignin aromatic ring skeleton to improving the flame retardant performance of EP. This strategy not only provides a novel method for flame retarding polymeric materials but also extends the comprehensive utilization of alkaline lignin.

Author statement

D.L., X.Z., P.D., X.L., H.G., H.Q., D.W., T.H., C.X. and H.M.R. performed experiments. D.L., X.Z., Z.L. and X.G. conceived research, analyzed data and wrote the manuscript with help from all the others. D. L. and X.Z. contributed equally to this work.

Declaration of competing interest

The authors declare that they have no known competing financial interests or personal relationships that could have appeared to influence the work reported in this paper.

Acknowledgments

This research was supported by financial supports from the National Natural Science Foundation of China (no.21774059), the Priority Academic Program Development (PAPD) of Jiangsu Higher Education Institutions, the opening funding of Jiangsu Key Lab of Biomass based Green Fuels and Chemicals.

References

[1] R. Auvergne, S. Caillol, G. David, B. Boutevin, J.P. Pascault, Biobased thermosetting epoxy: present and future, Chem. Rev. 114 (2014) 1082–1115, https://doi.org/10.1021/cr3001274.

[2] H. Gu, C. Ma, J. Gu, J. Guo, X. Yan, J. Huang, Q. Zhang, Z. Guo, An overview of multifunctional epoxy nanocomposites, J. Mater. Chem. C 4 (2016) 5890–5906, https://doi.org/10.1039/C6TC01210H.

[3] X.Y. Jian, Y. He, Y.D. Li, M. Wang, J.B. Zeng, Curing of epoxidized soybean oil with crystalline oligomeric poly(butylene succinate) towards high performance and sustainable epoxy resins, Chem. Eng. J. 326 (2017) 875–885, https://doi.org/10.1016/j.ce j.2017.06.039.

[4] J.T. Wan, Z.Y. Bu, C.J. Xu, B.G. Li, H. Fan, Preparation, curing kinetics, and properties of a novel low-volatile starlike aliphatic-polyamine curing agent for epoxy resins, Chem. Eng. J. 171 (2011) 357–367, https://doi.org/10.1016/j.cej.2011.04.004.

[5] J.M. Raquez, M. Deléglise, M.F. Lacrampe, P. Krawczak, Thermosetting (bio) materials derived from renewable resources: a critical review, Prog. Polym. Sci. 35 (2010) 487–509, https://doi.org/10.1016/j.progpolymsci.2010.01.001.

[6] J.H. Zhang, X.Q. Mi, S.Y. Chen, Z.J. Xu, D.H. Zhang, M.H. Miao, J.S. Wang, A bio-based hyperbranched flame retardant for epoxy resins, Chem. Eng. J. 381 (2020), 122719, https://doi.org/10.1016/j.cej.2019.122719.

[7] S.B. Wath, M.N. Katariya, S.K. Singh, G.S. Kanade, A.N. Vaidya, Separation of WPCBs by dissolution of brominated epoxy resins using DMSO and NMP: a comparative study, Chem. Eng. J. 280 (2015) 391–398, https://doi.org/10.1016/j.ce j.2015. 06.007.

[8] S. Khanal, W. Zhang, S. Ahmed, M. Ali, S. Xu, Effects of intumescent flame retardant system consisting of tris (2-hydroxyethyl) isocyanurate and ammonium polyphosphate on the flame retardant properties of high-density polyethylene composites, Compos. A Appl. Sci. Manufac. 112 (2018) 444–451, https://doi.org/10.1016/j.compositesa.2018.06.030.

[9] R.K. Jian, Y.F. Ai, L. Xia, L.J. Zhao, H.B. Zhao, Single component phosphamide-based intumescent flame retardant with potential reactivity towards low flammability and smoke epoxy resins, J. Hazard Mater. 371 (2019) 529–539, https://doi.org/10.1016/j.jhazmat.2019.03.045.

[10] P. Zhao, X. Gao, C. Lu, X. Wang, Y. He, D. Yao, Fabricating a partial wetting structure for improving the toughness of intumescent flame-retardant HDPE, J. Appl. Polym. Sci. 137 (2019) 48735, https://doi.org/10.1002/app.48735.

[11] A. Abdelkhalik, G. Makhlouf, M.A. Hassan, Manufacturing, thermal stability, and flammability properties of polypropylene containing new single molecule intumescent flame retardant, Polym. Adv. Technol. 30 (2019) 1403–1414, https://doi.org/10.1002/pat.4573.

[12] V.K. Thakur, M.K. Thakur, Recent advances in graft copolymerization and applications of chitosan: a review, ACS Sustain. Chem. Eng. 2 (2014) 2637–2652, https://doi.org/10.1021/sc500634p.

[13] G. Laufer, C. Kirkland, A.A. Cain, J.C. Grunlan, Clay–chitosan nanobrick walls: completely renewable gas barrier and flame-retardant nanocoatings, ACS Appl. Mater. Interfaces 4 (2012) 1643–1649, https://doi.org/10.1021/am2017915.

[14] T. Hosoya, H. Kawamoto, S. Saka, Role of methoxyl group in char formation from lignin-related compounds, J. Anal. Appl. Pyrolysis 84 (2009) 79–83, https://doi.org/10.1016/j.jaap.2008.10.024.

[15] H.T. Yang, B. Yu, X.D. Xu, S. Bourbigot, H. Wang, P.A. Song, Lignin-derived bio-based flame retardants toward high-performance sustainable polymeric materials, Green Chem. 22 (2020) 2129–2161, https://doi.org/10.1039/D0GC00449A.

[16] L.C. Cao, I.K.M. Yu, Y.Y. Liu, X.X. Ruan, C.W. Daniel, A.J. Tsang, Hunt, Y.S. Ok, H. Song, S.C. Zhang, Lignin valorization for the production of renewable chemicals: state-of-the-art review and future prospects, Bioresour. Technol. 269 (2018) 465–475, https://doi.org/10.1016/j.biortech.2018.08.065.

[17] A.R. Gonçalves, P. Benar, Hydroxymethylation and oxidation of Organosolv lignins and utilization of the products, Bioresour. Technol. 79 (2001) 103–111, https://doi.org/10.1016/S0960-8524(01)00056-6.

[18] J. Hu, R. Xiao, D.K. Shen, H.Y. Zhang, Structural analysis of lignin residue from black liquor and its thermal performance in thermogravimetric-Fourier transform infrared spectroscopy, Bioresour. Technol. 128 (2013) 633–639, https://doi.org/10.1016/j.biortech.2012.10.148.

[19] A. Kumar, A. Kumar, J. Kumar, T. Bhaskar, Catalytic pyrolysis of soda lignin over zeolites using pyrolysis gas chromatography-mass spectrometry, Bioresour. Technol. 291 (2019) 121822, https://doi.org/10.1016/j.biortech.2019.121822.

[20] M.P. Pandey, C.S. Kim, Lignin depolymerization and conversion: a review of thermochemical methods, Chem. Eng. Technol. 34 (2011) 29–41, https://doi.org/10.1002/ceat.201000270.

[21] B. Li, X.C. Zhang, R.Z. Su, An investigation of thermal degradation and charring of larch lignin in the condensed phase: the effects of boric acid, guanyl urea phosphate, ammonium dihydrogen phosphate and ammonium polyphosphate, Polym. Adv. Technol. 1 (2002) 35–44, https://doi.org/10.1016/S0141-3910(01)00202-6.

[22] A. Gregorova, R. Kosikova, R. Moravcik, Stabilization effect of lignin in natural rubber, Polym. Degrad. Stabil. 91 (2006) 229–233, https://doi.org/10.1016/j.polym degradstab.2005.05.009.

[23] L.N. Liu, G.B. Huang, P.A. Song, Y.M. Yu, S.Y. Fu, Converting industrial alkali lignin to biobased functional additives for improving fire behavior and smoke suppression of polybutylene succinate, ACS Sustain. Chem. Eng. 4 (2016) 4732–4742, https://doi.org/10.1021/acssuschemeng.6b00955.

[24] L.N. Liu, M.B. Qian, P.A. Song, G.B. Huang, Y.M. Yu, S.Y. Fu, Fabrication of green lignin-based flame retardants for enhancing the thermal and fire retardancy properties of polypropylene/wood composites, ACS Sustain. Chem. Eng. 4 (2016) 2422–2431, https://doi.org/10.1021/acssuschemeng.6b00112.

[25] W. Wu, H.B. He, T. Liu, R.C. Wei, X.W. Cao, Q.J. Sun, S. Venkatesh, R.K.K. Yuen, V. A.L. Roy, R.K.Y. Li, Synergetic enhancement on flame retardancy by melamine phosphate modified lignin in rice husk ash filled P34HB biocomposites, Compos. Sci. Technol. 168 (2018) 246–254, https://doi.org/10.1016/j.compscitech.2018.09.024.

[26] L. Costes, F. Laoutid, M. Aguedo, A. Richel, S. Brohez, C. Delvosalle, P. Dubois, Phosphorus and nitrogen derivatization as efficient route for improvement of lignin flame retardant action in PLA, Eur. Polym. J. 84 (2016) 652–667, https://doi.org/10.1016/j.eurpolymj.2016.10.003.

[27] T. Yoshida, Z.Y. Xia, K. Takeda, T. Katsuta, K. Sugimoto, M. Funaoka, Peroxidase-catalyzed polymerization and copolymerization of lignin-based macromonomer (lignocresol) having high content of p-cresol and thermal properties of the resulting polymers, Polym. Adv. Technol. 16 (2005) 783–788, https://doi.org/10.1002/pat.6 21.

[28] W.J. Gao, J.P.W. Inwood, P. Fatehi, Sulfonation of phenolated kraft lignin to produce water soluble products, J. Wood Chem. Technol. 39 (2019) 225–241, https://doi.org/10.1080/02773813.2019.1565866.

[29] Y. Matsushita, H. Sano, M. Imai, T. Imai, K. Fukushima, Phenolization of hardwood sulfuric acid lignin and comparison of the behavior of the syringyl and guaiacyl units in lignin, J. Wood Sci. 53 (2007) 67–70, https://doi.org/10.1007/s10086-006-0814-3.

[30] D. Kai, M.J. Tan, P.L. Chee, Y.K. Chua, Y.L. Yap, X.J. Loh, Towards lignin-based functional materials in a sustainable world, Green Chem. 18 (2016) 1175–1200, https://doi.org/10.1039/C5GC02616D.

[31] F. Ferdosian, Z.S. Yuan, M. Anderson, C.C. Xu, Thermal performance and thermal decomposition kinetics of lignin-based epoxy resins, J. Anal. Appl. Pyrolysis 119 (2016) 124–132, https://doi.org/10.1016/j.jaap.2016.03.009.

[32] V. Vasudev, X.L. Ku, J.Z. Lin, Kinetic study and pyrolysis characteristics of algal and lignocellulosic biomasses, Bioresour. Technol. 288 (2019), 121496, https://doi.org/10.1016/j.biortech.2019.121496.

[33] K. Qin, H. Thunman, Diversity of chemical composition and combustion reactivity of various biomass fuels, Fuel 147 (2015) 161–169, https://doi.org/10.1016/j.fuel.2015.01.047.

[34] S. Vyazovkin, A.K. Burnhan, J.M. Criado, L.A. Perez-Maqueda, C. Popescu, N. Sbirrazzuoli, ICTAC Kinetics Committee recommendations for performing kinetic computations on thermal analysis data, Thermochim. Acta 520 (2011) 1–19, https://doi.org/10.1016/j.tca.2020.178597.

[35] S.R. Wang, B. Ru, H.Z. Lin, W.X. Sun, Z.Y. Luo, Pyrolysis behaviors of four lignin polymers isolated from the same pine wood, Bioresour. Technol. 182 (2015) 120–127, https://doi.org/10.1016/j.biortech.2015.01.127.

[36] G.J. Jiao, P. Peng, S.L. Sun, Z.C. Geng, D. She, Amination of biorefinery technical lignin by Mannich reaction for preparing highly efficient nitrogen fertilizer, Int. J. Biol. Macromol. 127 (2019) 544–554, https://doi.org/10.1016/j.ijbiomac.2019.01.0 76.

[37] X.D. Jin, J. Sun, J.S.Q. Zhang, X.Y. Gu, S. Bourbigot, H.F. Li, W.F. Tang, S. Zhang, Preparation of a novel intumescent flame retardant based on supramolecular interactions and its application in polyamide 11, ACS Appl. Mater. Interfaces 9 (2017) 24964–24975, https://doi.org/10.1021/acsami.7b06250.

[38] Y. Gao, C. Deng, Y. Du, S. Huang, Y. Wang, A novel bio-based flame retardant for polypropylene from phytic acid, Polym. Degrad. Stabil. 161 (2019) 298–308, https://doi.org/10.1016/j.polymdegradstab.2019.02.005.

[39] Y.H. Guan, J.Q. Huang, J.C. Yang, Z.B. Shao, Y.Z. Wang, An effective way to flame-retard biocomposite with ethanolamine modified ammonium polyphosphate and its flame retardant mechanisms, Ind. Eng. Chem. Res. 54 (2015) 3524–3531, https://doi.org/10.1021/acs.iecr.5b00123.

[40] Z.B. Shao, C. Deng, Y. Tan, M.J. Chen, L. Chen, Y.Z. Wang, An efficient mono-component polymeric intumescent flame retardant for polypropylene: preparation and application, ACS Appl. Mater. Interfaces 6 (2014) 7363–7370, https://doi.org/10.1021/am500789q.

[41] G.S. Liu, W.Y. Chen, J.G. Yu, A novel process to prepare ammonium polyphosphate with crystalline form II and its comparison with melamine polyphosphate, Ind. Eng. Chem. Res. 49 (2010) 12148, https://doi.org/10.1021/ie 1014102.

[42] X.S. Chen, Y.H. Ma, Y.J. Cheng, A.Q. Zhang, W. Liu, Enhanced mechanical and flame-resistant properties of polypropylene nanocomposites with reduced graphene oxide-functionalized ammonium polyphosphate and pentaerythritol, J. Appl. Polym. Sci. 136 (2019) 48036, https://doi.org/10.1002/app.48036.

[43] Y.Q. Xiong, Z.J. Jiang, Y.Y. Xie, X.Y. Zhang, W.J. Xu, Development of a DOPO-containing melamine epoxy hardeners and its thermal and flame-retardant properties of cured products, J. Appl. Polym. Sci. 127 (2013) 4352–4358, https://doi.org/10.1002/app.37635.

[44] L. Costes, F. Laoutid, S. Brohez, C. Delvosalle, P. Dubois, Phytic acid–lignin combination: a simple and efficient route for enhancing thermal and flame retardant properties of polylactide, Eur. Polym. J. 94 (2017) 270–285, https://doi.org/10.1016/j. eurpolymj.2017.07.018.

[45] C.S. Wu, Y.L. Liu, Y.C. Chiu, Y.S. Chiu, Thermal stability of epoxy resins containing flame retardant components: an evaluation with thermogravimetric analysis, Polym. Degrad. Stabil. 7 (2002) 41–48, https://doi.org/10.1016/S0141-3910(02)00117-9.

[46] Y. Tan, Z.B. Shao, L.X. Yu, J.W. Long, M. Qi, L. Chen, Y.Z. Wang, Piperazine-modified ammonium polyphosphate as monocomponent flame-retardant hardener for epoxy resin: flame retardance, curing behavior and mechanical property, Polym. Chem. 7 (17) (2016) 3003–3012, https://doi.org/10.1039/C6PY00434B.

[47] Y.Q. Shi, B. Yu, Y.Y. Zheng, J. Yang, Z.P. Duan, Y. Hu, Design of reduced graphene oxide decorated with DOPO-phosphanomidate for enhanced fire safety of epoxy

resin, J. Colloid Interface Sci. 521 (2018) 160–171, https://doi.org/10.1016/j.jcis.2018.02.054.
[48] Q. Wu, B. Qu, Synergistic effects of silicotungstic acid on intumescent flame-retardant polypropylene, Polym. Degrad. Stabil. 74 (2001) 255–261, https://doi.org/10.1016/S0141-3910(01)00155-0.
[49] Z.Q. Ma, J.H. Wang, H.Z. Zhou, Y. Zhang, Y.Y. Yang, X.H. Liu, J.W. Ye, D.Y. Chen, S.R. Wang, Relationship of thermal degradation behavior and chemical structure of lignin isolated from palm kernel shell under different process severities, Fuel Process. Technol. 181 (2018) 142–156, https://doi.org/10.1016/j.fuproc.2018.09.020.
[50] D. Aimacana, L. Quiles-carrillo, R. Balart, T. Boronat, N. Montanes, Kinetic analysis of the curing of a partially biobased epoxy resin using dynamic differential scanning calorimetry, Polymers 11 (2019) 391, https://doi.org/10.3390/polym11030391.
[51] F. Ferdosian, Z.S. Yuan, M. Anderson, C.C. Xu, Thermal performance and thermal decomposition kinetics of lignin-based epoxy resins, J. Anal. Appl. Pyrolysis 119 (2016) 124–132, https://doi.org/10.1016/j.jaap.2016.03.009.
[52] Z.Q. X, Y. Zhang, X.Y. Du, P.A. Song, Z.P. Fang, Green and scalable fabrication of Core−Shell biobased flame retardants for reducing flammability of polylactic acid, ACS Sustain. Chem. Eng. 7 (2019) 8954–8963, https://doi.org/10.1021/acssuschemeng.9b01016.
[53] T. Zhang, H.Q. Yan, L. Shen, Z.P. Fang, J.J. Wang, B.Y. Zhang, Chitosan/Phytic acid polyelectrolyte complex: a green and renewable intumescent flame retardant system for ethylene–vinyl acetate copolymer, Ind. Eng. Chem. Res. 53 (2014) 19199–19207, https://doi.org/10.1021/ie503421f.
[54] Z.Q. Ma, Q.F. Sun, J.W. Ye, Q.F. Yao, C. Zhao, Study on the thermal degradation behaviors and kinetics of alkali lignin for production of phenolic-rich bio-oil using TGA-FTIR and Py–GC/MS, J. Anal. Appl. Pyrolysis 117 (2016) 116–124, https://doi.org/10.1016/j.jaap.2015.12.007.
[55] D.K. Shen, G.F. Liu, J. Zhao, J.T. Xue, S.P. Guan, R. Xiao, Thermo-chemical conversion of lignin to aromatic compounds: effect of lignin source and reaction temperature, J. Anal. Appl. Pyrolysis 112 (2015) 56–65, https://doi.org/10.1016/j.jaap.2015.02.022.